华中师范大学
CENTRAL CHINA NORMAL UNIVERSITY

Nuclear Structure Effects to High-Precision Spectroscopy in Hydrogen-Like Atoms

Chen Ji

Institute of Particle Physics
Central China Normal University

High Energy Theory Forum
Beijing 2024.03.13

Nuclear structures from spectroscopy

- Precision spectroscopy provides abundant information on nuclear structures.

Nuclear structure observables

Nuclear spin
Charge radius
Magnetic dipole moment
electric quadrupole moment
magnetic radius

Nuclear structure physics

Nuclear shell evolution
New β stability line, neutron-rich drip line
Halo structure of radioactive nuclei
Internal nucleon distribution
Nuclear deformation

- Precision measurements on nuclear structures provides crucial guidance to building nuclear Hamiltonian models and nuclear many-body theories
  - Deuteron quadrupole moment $\rightarrow$ nuclear tensor force
  - Magnetic moment/radius $\rightarrow$ meson-exchange current
  - Charge radii for $A \geq 3$ systems $\rightarrow$ three-nucleon force

Precision Spectroscopy in Radioactive Nuclides

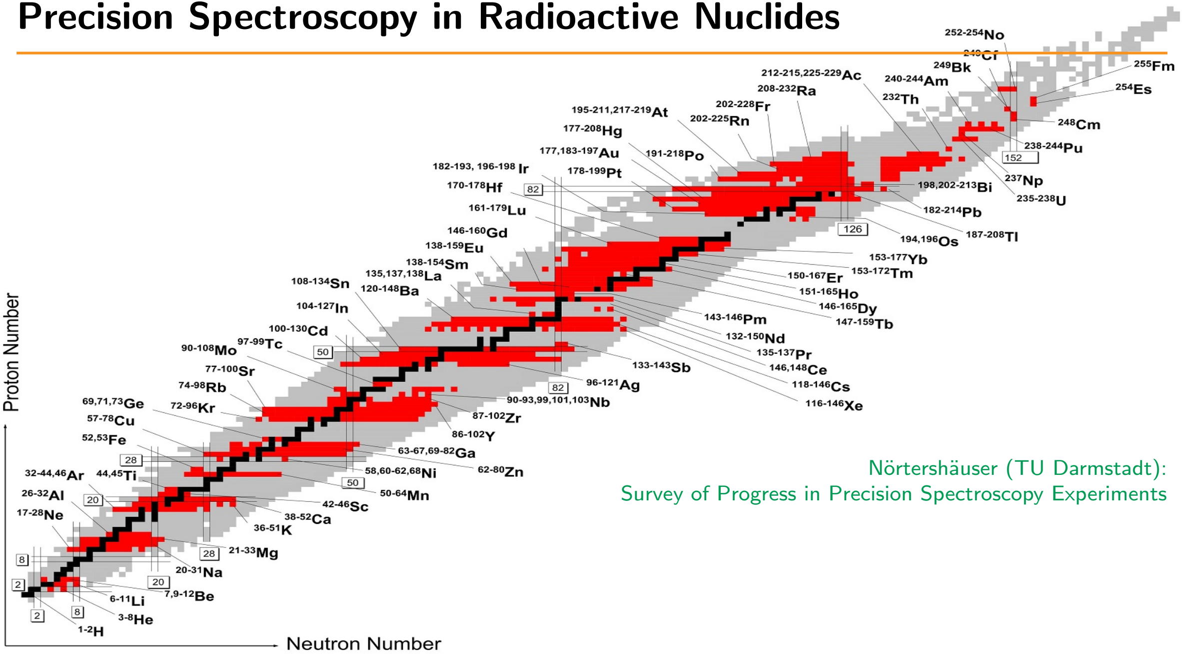

Nörtershäuser (TU Darmstadt):
Survey of Progress in Precision Spectroscopy Experiments

Proton radius puzzle

- electron-proton interaction experiments: $r_p = 0.8770(45)$ fm
  - eH spectroscopy
  - $e{-}p$ scattering
- μ-p interaction experiments: $r_p = 0.8409(4)$ fm
  - μH Lamb shift (ΔE_{2S-2P}) [PSI-CREMA]
    Pohl *et al.*, Nature (2010); Antognini *et al.*, Science (2013)

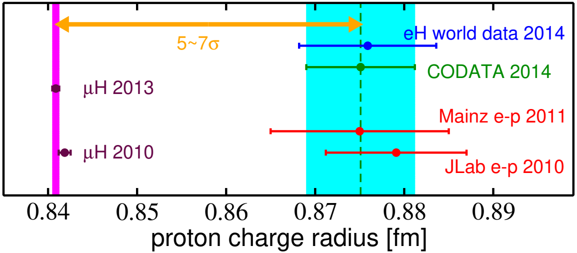

Origin of the discrepancy?

- Search for the origin of the radius puzzle
  - Lepton universality violation?
  - Exotic hadron structure?
  - Under-estimated experimental uncertainties in eH and e-p?

These explanations are still in debate...

Lepton universality violation?

Physics beyond standard model

- new force carrier, e.g., dark photon: couples differently with e and μ
- explain both the r_p puzzle & $(g-2)_\mu$ puzzle

Tucker-Smith, Yavin, PRD 83 (2011) 101702
Batell, McKeen, Pospelov, PRL 107 (2011) 011803
Barger, Chiang, Keung, Marfatia, PRL 106 (2011) 153001
Endo, Hamaguchi, Mishima, PRD 86 (2012) 095029

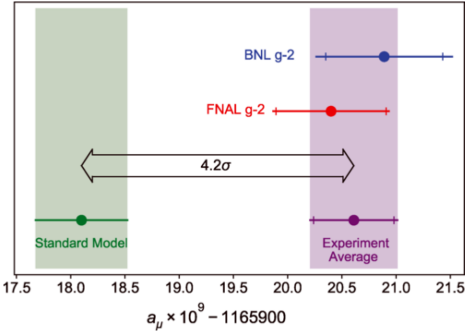

$(g-2)_\mu$ collaboration, PRL 126 (2021) 141801

Error in ep scattering experiment (analysis)?

- $G_E^p(Q^2) = 1 - \frac{1}{6}\, \boldsymbol{r_p^2}\, Q^2 + \ldots$
- Q^2 not small enough / floating normalization

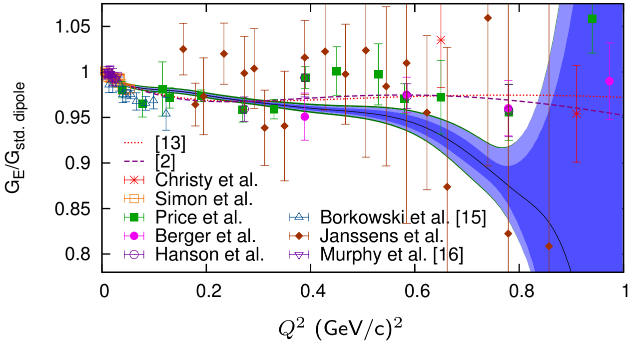

- dispersion analysis on n/p EM form factors: $r_p = 0.84(1)$ fm

Lorenz, Hammer, Meißner, EPJA 48 (2012) 151

Lorenz, Hammer, Meißner, Dong, PRD 91 (2015) 014023

- deficiency in radiative correction model:

Lee, Arrington, Hill, PRD 92 (2015) 013013

Underestimated uncertainties in eH spectroscopies?

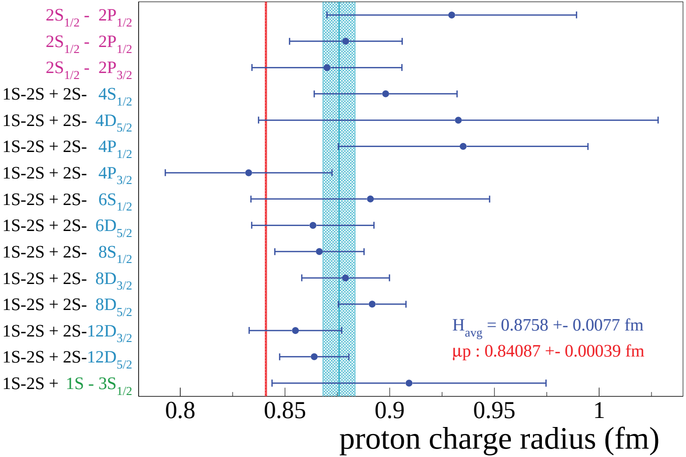

Phol *et al.*, Annu. Rev. Nucl. Part. Sci 63 (2013) 175

- large uncertainty in individual eH measurement
- correlated measurements?

Solve the radius puzzle

- New experiment to measure the proton radius
  - $e - p$ scattering (JLab, Mainz, Tohoku U.)
  - $\mu - p$ scattering (PSI-MUSE)
  - hydrogen spectroscopy (MPQ, LKB, York U.)

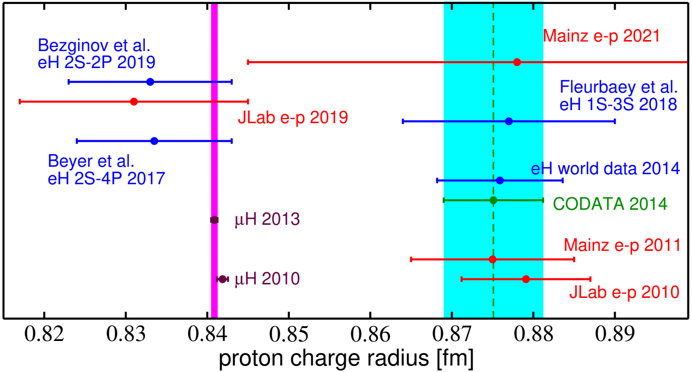

We seem to better (not fully) understand the proton radius now.

Electron scattering on light nuclei

- Traditional nuclear theory is based on independent particle models (IPM)
- IPM poorly describes short-range nucleon-nucleon correlation and exotic nuclear structure
- Electron Scattering (ES) provides a clean way to probe nuclear structure and spectrum
- Precise Electromagnetic probes give accurate constraints on nucleon-nucleon interaction and meson-exchange current

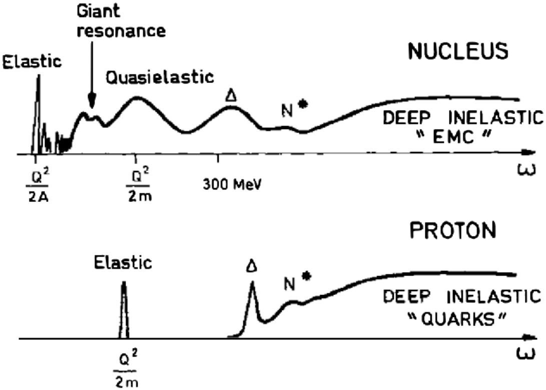

Elastic electron scattering and nuclear form factors

- Elastic electron-nucleus scattering provides information on nuclear charge, quadrupole, magnetic structures

$$\frac{d\sigma(E,\theta)}{d\Omega}^{PWIA} = \sigma_{Mott}(E,\theta)[A(q) + B(q)tan(\theta/2)^2]$$

$$A(q) = F_{C0}(q)^2 + (M_d^2 Q_d)^2 \frac{8}{9}\eta^2 F_{C2}^2(q) + (\frac{M_d}{M_p}\mu_d)^2 \frac{2}{3}\eta(1+\eta) F_{M1}^2(q)$$

$$B(q) = (\frac{M_d}{M_p}\mu_d)^2 \frac{4}{3}\eta(1+\eta)^2 F_{M1}^2(q) \qquad \eta = q^2/(4M_d^2)$$

- scattering on light nuclei were intensively studied during 1960-1980
- Most recent measurements were done at Jefferson Lab and Mainz Microtron (light stable nuclei)

Reviews:
Frois, Papanicolas, Ann. Rev. Nucl. Part. Sci. 37, 133 (1987)
Hofstadter, Rev. Mod. Phys. 28, 214 (1956)
Sick, Prog. Part. Nucl. Phys. 47, 245 (2001); arXiv:1505.06924

New electron scattering experimental plan

- JLab & Mainz: measure G_E and G_M for light nuclei at low Q^2
  - ep scattering (JLab PRad: Xiong et al., Nature 575, 147 (2019)
  - $e-{}^2$H scattering (JLab DRad: improve precision by a factor of 2)
  - $e-{}^3$H & e^3He scattering

Experiments Proposal:
Mainz A1: wwwa1.kph.uni-mainz.de/experiments-and-accepted-proposals/
JLab Hall A: www.jlab.org/physics/experiments

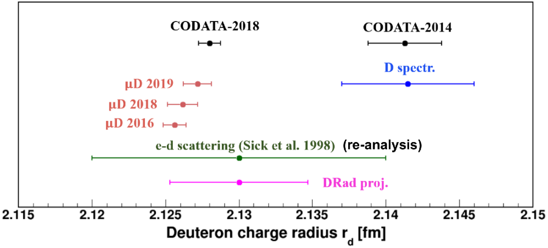

New electron scattering experimental plan

- JLab & Mainz: measure G_E and G_M for light nuclei at low Q^2
  - ep scattering (JLab PRad: Xiong et al., Nature 575, 147 (2019)
  - $e-{}^2$H scattering (JLab DRad: improve precision by a factor of 2)
  - $e-{}^3$H & e^3He scattering

Experiments Proposal:
Mainz A1: wwwa1.kph.uni-mainz.de/experiments-and-accepted-proposals/
JLab Hall A: www.jlab.org/physics/experiments

- SCRIT (RIKEN) & ELISe (GSI-FAIR): electron scattering on exotic nuclei

Suda, Wakasugi, Prog. Part. Nucl. Phys 55, 417 (2005)

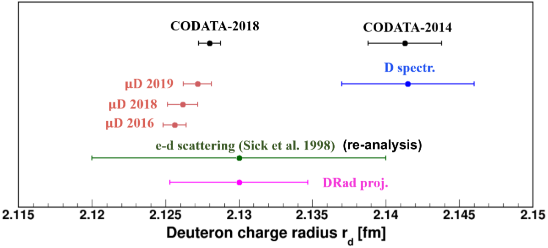

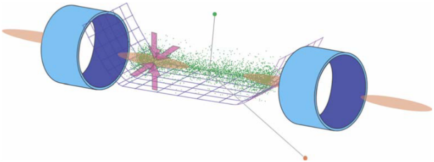

Spectroscopy measurement of nuclear radii in other atoms

- Lamb shift in muonic atoms/ions (PSI-CREMA)
  - $\mu^2\mathrm{H}$ [Pohl *et al.*, Science 2016]
  - $\mu^4\mathrm{He}^+$ [Krauth *et al.*, Nature 2021]
  - $\mu^3\mathrm{He}^+$ [K. Schuhmann *et al.*, arXiv:2305.11679]
  - μLi, μBe, μB [PSI-QUARTET: X-ray transition]

Nuclear charge radii

- $e^{3,4}$He spectroscopy

^{3}He-^{4}He charge-radius isotope-shift

- hyperfine splitting in muonic measurements (PSI-CREMA)
  - $\mu^2\mathrm{H}$, $\mu^3\mathrm{He}^+$ [In plan]

Nuclear magnetic Zemach radius

Theoretical studies of nuclear structure

- Nuclear theory has made great progress in the past 30 years
- microscopic nucelon-nucleon interaction development
- microscopic nucleon electroweak interaction development
- quantum many-body calculations (ab initio) make accurate study of nuclear structure and reaction possible
- Recent development can make rigorous uncertainty quantification in theoretical predictions

Phenomenological potential

- **Argonne v_{18}** fitted to
  - 1787 pp & 2514 np observables for $E_{lab} \leq 350$ MeV with $\chi^2/\mathrm{datum} = 1.1$
  - nn scattering length & ^{2}H binding energy

- **Urbana IX**

$$V_{ijk} = V_{ijk}^{2\pi P} + V_{ijk}^{R}$$

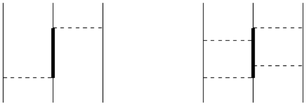

Phenomenological potentials

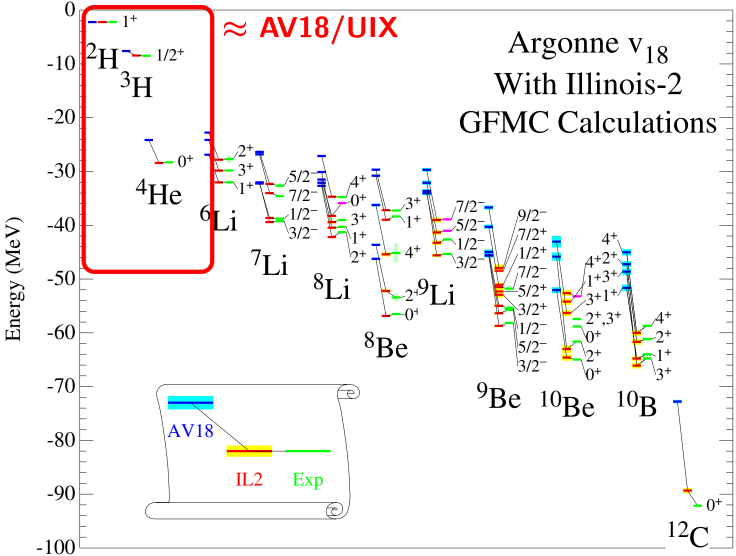

Chiral effective field theory potential

- **effective theory**
  of low-energy QCD

- **nuclear forces**
  are built in systematic expansions
  of Q/Λ_χ

- **coupling constants**
  fitted to nuclear data

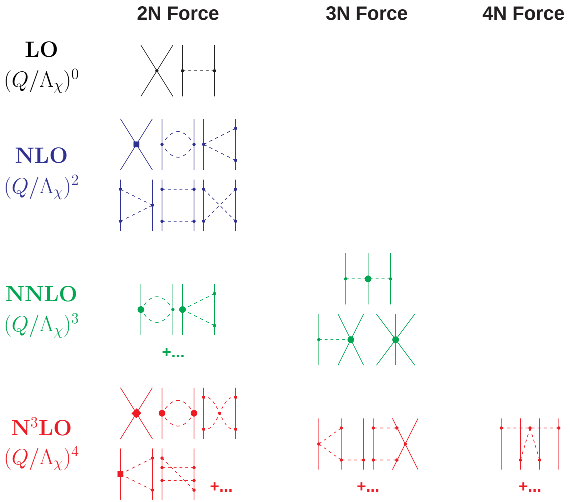

Chiral effective field theory potential

- Chiral EFT determination of nuclear binding energies and charge radii

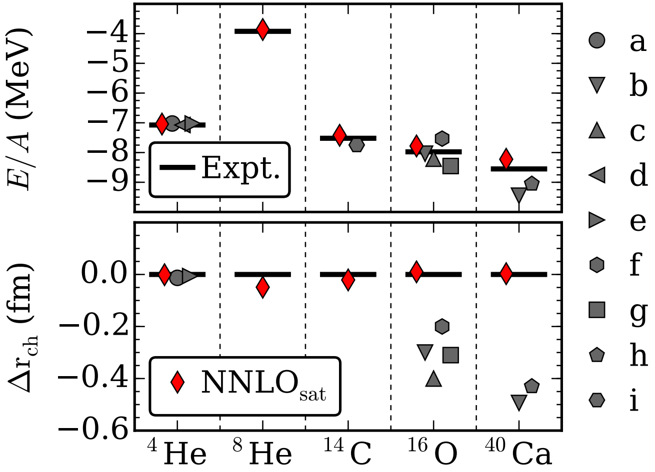

Ekström et al., Phys. Rev. C 91, 051301 (2015)

Progress in ab initio nuclear structure theories

- Advances in ab initio calculations made nuclear chart accessible

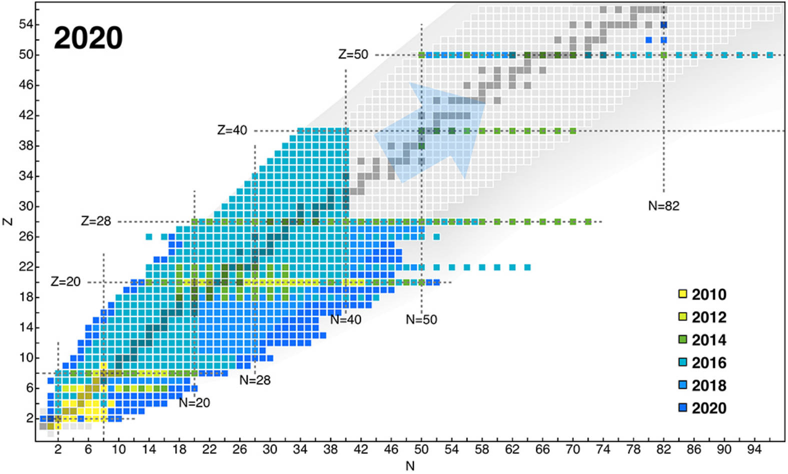

Hergert, Front. Phys. 8, 379 (2020)

Current understanding of nuclear structure

- Both experiments and theories have made great progress in understanding nuclear structures
- However, discrepancies appear at precision levels
  - discrepancies among experiments
  - disagreement between experiments and theories
  - theories face challenges in accurately describing exotic structures

The ^{2}H radius puzzle

- $\mu^2\mathrm{H}$ Lamb shift: $r_d = 2.12562(78)$ fm   Pohl, *et al.*, Science 353, 669 (2016)
- CODATA-2014: $r_d = 2.1415(45)$ fm

- isotope shift $r_d^2 - r_p^2$:
  $\delta(\mu^2\mathrm{H}, \mu\mathrm{H}) = 3.8112(34)$ fm^2
  $\delta(e^2\mathrm{H}, e\mathrm{H}) = 3.8201(07)$ fm^2 Parthey, *et al.*, PRL (2010)

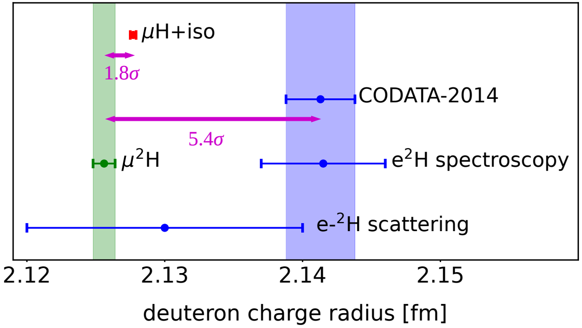

^{2}H charge & magnetic form factors

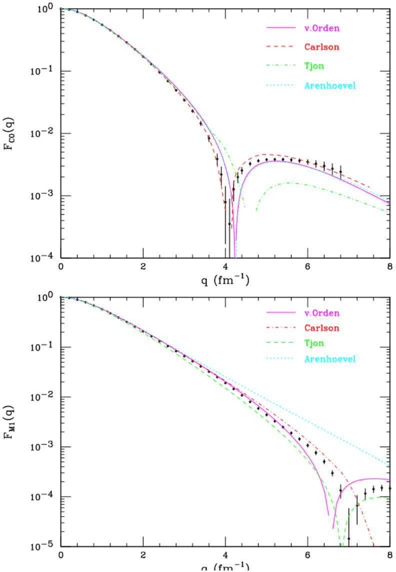

- ^{2}H $G_C(q)$:
  better agreement between theory & data
- ^{2}H $G_M(q)$:
  less agreement between theory & data

Sick, arXiv:1505.06924

The helium isotope shift puzzle

- Discrepancies in ^{3}He-^{4}He charge radius isotope shift measurements

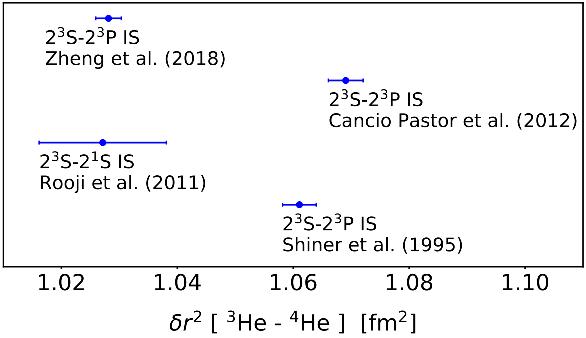

Zheng, et al., Phys. Rev. Lett. 119, 263002 (2017)
Cancio Pastor, et al., Phys. Rev. Lett. 108, 143001 (2012)
van Rooij, et al., Science 333, 196 (2011)
Shiner, et al. Phys. Rev. Lett. 74, 3553 (1995)

^{3}He charge & magnetic form factors

- ^{3}H $G_C(q)$:
  better agreement between theory & data
- ^{3}H $G_M(q)$:
  less agreement between theory & data

Sick, arXiv:1505.06924

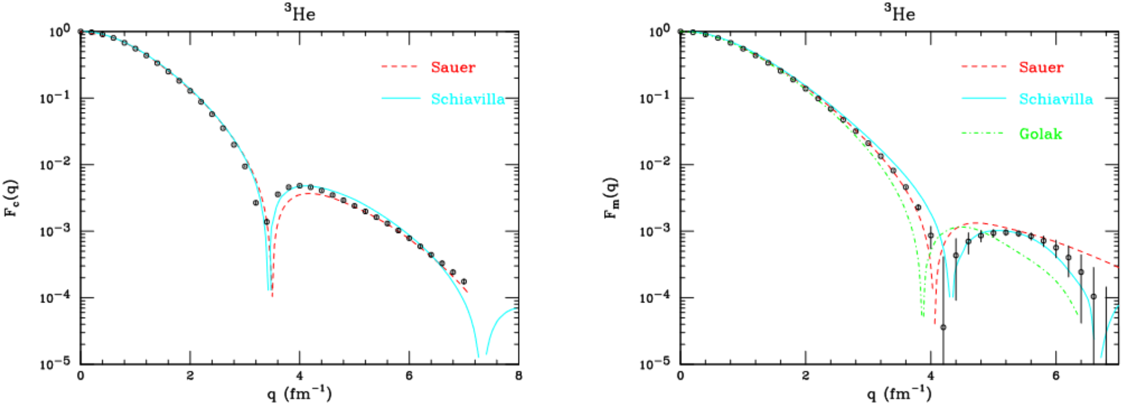

Spectroscopy and charge radii of ^{6,8}He

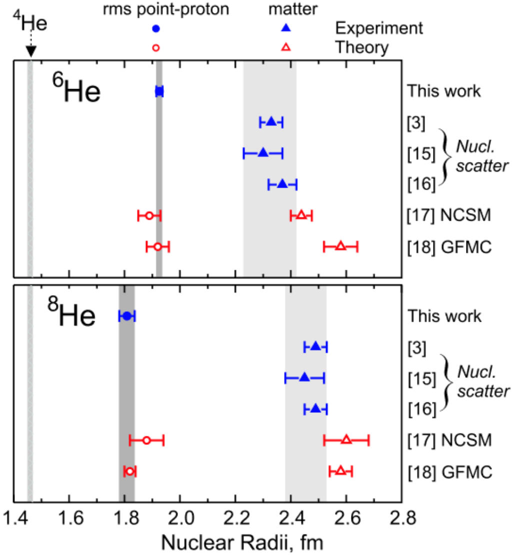

- difference between experiments and theories indicate discrepancies in the description of halo structures in ^{6,8}He

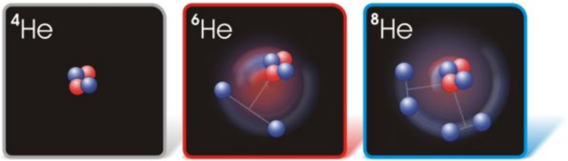

Wang et al., Phys. Rev. Lett. 93, 142501 (2004)
Muller et al., Phys. Rev. Lett. 99, 252501 (2007)

The lithium magnetic Zemach radius puzzle

- magnetic Zemach radius indicates nuclear magnetic distribution
- R_z discrepancies in spectroscopy and scattering experiments

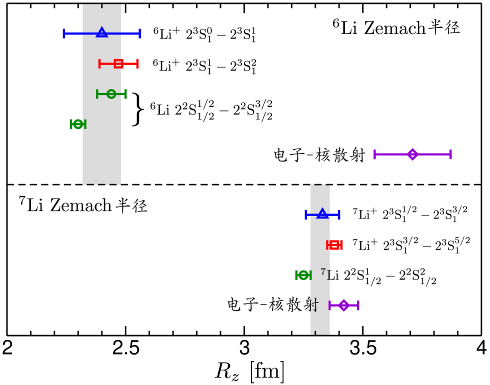

Puchalski, Pachucki, PRL 111, 243001 (2013)
Qi et al., PRL 125, 183002 (2020)
Li et al., PRL 124, 063002 (2020)
Guan et al., PRA 102, 030801(R) (2020)

Spectroscopy and Li isotopes charge radii

- cluster configuration in ^{6,7}Li
- halo structures in ^{11}Li
- disagreement between ab initio theory and data

TRIUMF & GSI:
Phys. Rev. Lett. 93, 113002 (2004); Phys. Rev. C 84, 024307 (2011);
Phys. Rev. A 83, 012516 (2011)

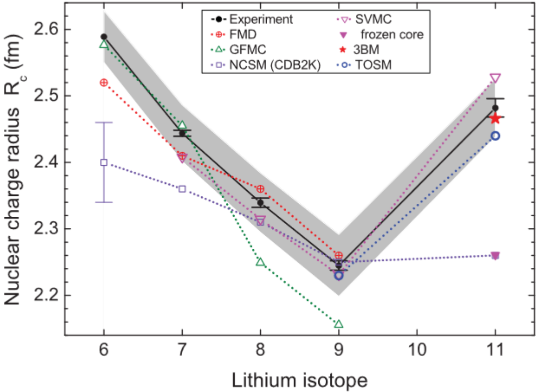

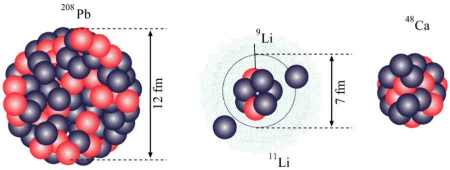

Challenges in nuclear structure studies

- precision spectroscopy brings nuclear structure study into precision era
- electromagnetic probes provides important information to improve nuclear potentials and ab initio theories

μH Lamb shift experiment

Lamb Shift: 2S-2P splitting in atomic spectrum   Pic: Pohl *et al.* Nature (2010)

- **prompt X-ray ($t \sim 0$s):** μ^- stopped in H_2 gases

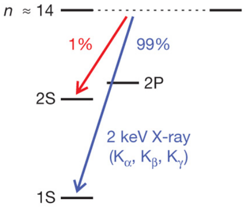

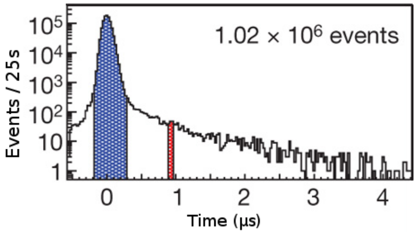

μH Lamb shift experiment

Lamb Shift: 2S-2P splitting in atomic spectrum   Pic: Pohl *et al.* Nature (2010)

- **prompt X-ray ($t \sim 0\mathrm{s}$):** μ^- stopped in H_2 gases

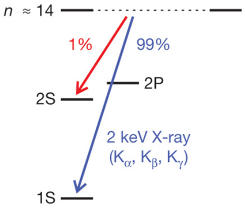

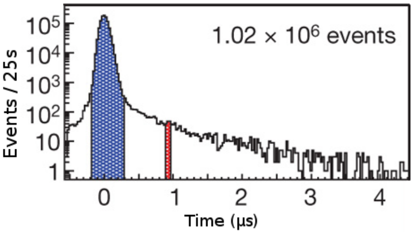

- **delayed X-ray ($t \sim 1\mu\mathrm{s}$):** laser induced 2S$\rightarrow$2P

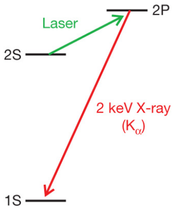

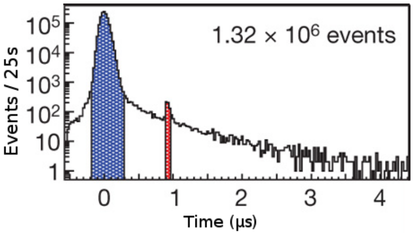

μH Lamb shift experiment

- measure $K_\alpha^{\text{delayed}} / K_\alpha^{\text{prompt}}$
- $\delta E_{LS} = h f_{res}$

Pic: Pohl *et al.* Nature (2010)

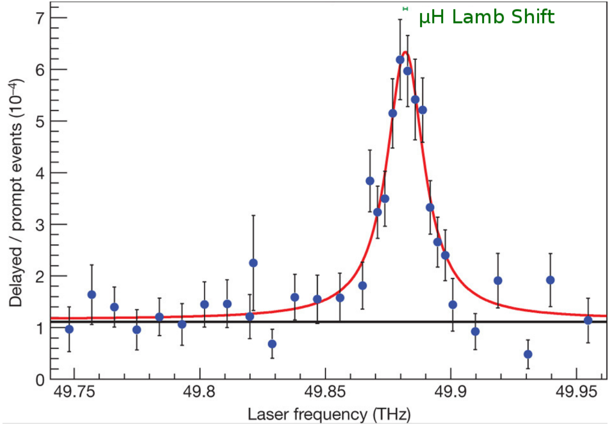

Nuclear structure effects to Lamb shift

- Extract nuclear charge radius from Lamb shift in muonic atoms

$$\delta E_{\mathrm{LS}} = \delta_{\mathrm{QED}} + \mathcal{A}_{\mathrm{OPE}}\, R_E^2 + \delta_{\mathrm{TPE}}$$

Nuclear structure effects to Lamb shift

- Extract nuclear charge radius from Lamb shift in muonic atoms

$$\delta E_{\mathrm{LS}} = \delta_{\mathrm{QED}} + \mathcal{A}_{\mathrm{OPE}}\, R_E^2 + \delta_{\mathrm{TPE}}$$

- **QED effects**
  - Vacuum polarization (Uehling effect)
  - Lepton self energy
  - relativistic recoil

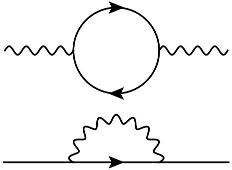

Nuclear structure effects to Lamb shift

- Extract nuclear charge radius from Lamb shift in muonic atoms

$$\delta E_{\rm LS} = \delta_{\rm QED} + \mathcal{A}_{\rm OPE}\, R_E^2 + \delta_{\rm TPE}$$

- **Nuclear structure effects**

Nuclear structure effects to Lamb shift

- Extract nuclear charge radius from Lamb shift in muonic atoms

$$\delta E_{\mathrm{LS}} = \delta_{\mathrm{QED}} + \boxed{\mathcal{A}_{\mathrm{OPE}}\, R_E^2} + \delta_{\mathrm{TPE}}$$

- **Nuclear structure effects**
  - $\propto R_E^2 \Longrightarrow$ **one-photon exchange (OPE)**
    $\mathcal{A}_{\mathrm{OPE}} \approx m_\mu^3 (Z\alpha)^4/12$

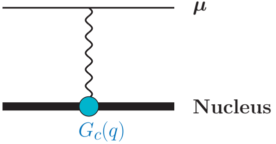

Nuclear structure effects to Lamb shift

- Extract nuclear charge radius from Lamb shift in muonic atoms

$$\delta E_{\rm LS} = \delta_{\rm QED} + \mathcal{A}_{\rm OPE}\, R_E^2 + \boxed{\delta_{\rm TPE}}$$

- **Nuclear structure effects**
  - $\boldsymbol{\delta_{\rm TPE}} \Longrightarrow$ **two-photon exchange (TPE)**
    - elastic part: Zemach moment $\delta_{\rm Zem}$
    - inelastic part: nuclear polarizability $\delta_{\rm pol}$

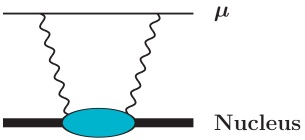

Nuclear structure effects to Lamb shift

- Extract nuclear charge radius from Lamb shift in muonic atoms

$$\delta E_{\rm LS} = \delta_{\rm QED} + \mathcal{A}_{\rm OPE}\, R_E^2 + \boxed{\delta_{\rm TPE}}$$

- **Nuclear structure effects**
  - $\boldsymbol{\delta_{\rm TPE}} \Longrightarrow$ **two-photon exchange (TPE)**
    - elastic part: Zemach moment $\delta_{\rm Zem}$
    - inelastic part: nuclear polarizability $\delta_{\rm pol}$

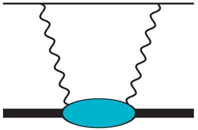

- **The accuracy of extracting R_E relies on the theoretical input of $\delta_{\rm TPE}$**

  μ^2H experiment: $\delta_{\rm pol}$ requires 1% accruacy
  $\mu^{3,4}$He$^+$ experiment: $\delta_{\rm pol}$ requires 5% accuracy

Nuclear polarizability from sum rules for photo-nuclear reactions

$$\delta_{\rm pol} = \sum_{g,\, S_{\hat{O}}} \int_{\omega_{th}}^{\infty} d\omega \, \underbrace{g(\omega)}_{\text{weight}} \, \underbrace{S_{\hat{O}}(\omega)}_{\text{response function}}$$

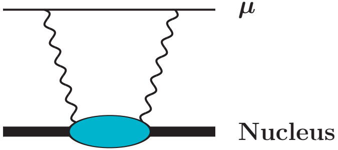

- energy-weighted sum rules $g(\omega)$
- nuclear response function $S_{\hat{O}}(\omega)$

$$S_O(\omega) = \sum\!\!\!\!\!\!\int_f |\langle\psi_f|\hat{O}|\psi_0\rangle|^2 \delta(E_f - E_0 - \omega)$$

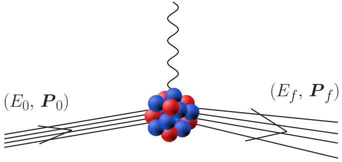

Nuclear polarizability from sum rules for photo-nuclear reactions

$$\delta_{\rm pol} = \sum_{g,\,S_{\hat{O}}} \int_{\omega_{th}}^{\infty} d\omega \; \underbrace{g\left(\omega\right)}_{\text{weight}} \; \underbrace{S_{\hat{O}}\left(\omega\right)}_{\text{response function}}$$

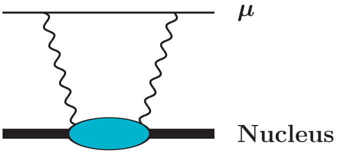

Contributing terms in nuclear polarizability $\delta_{\rm pol}$:

- multipole expansion to EM operators
  - E0, E1, E2, M1 response sum rules
- relativistic and Coulomb-distortion corrections
- intrinsic nucleon structure corrections

CJ, Bacca, Barnea, Hernandez, Nevo-Dinur, JPG 45 (2018) 093002

Nuclear response function: continuum spectrum

- The nucleus is virtually excited during the TPE process

$$S_O(\omega) = \sum_f |\langle \psi_f | \hat{O} | \psi_0 \rangle|^2 \delta(E_f - E_0 - \omega)$$

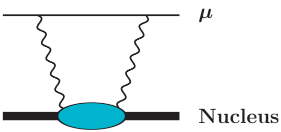

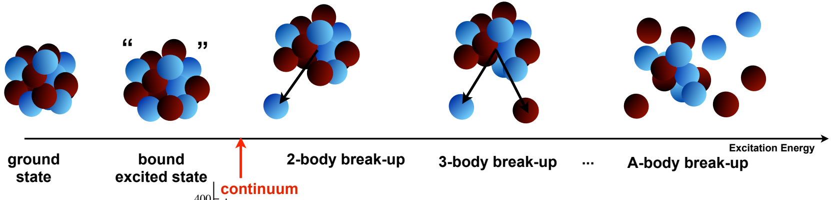

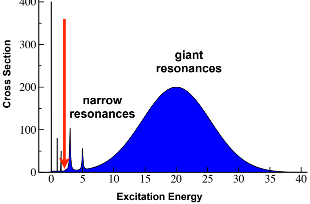

$$\sigma \propto \left| \langle \Psi_f | J^\mu | \Psi_0 \rangle \right|^2$$

Exact knowledge limited in energy and mass number

Determine $S_{\hat{O}}$ from photo-nuclear reaction experiments

$$\sigma_\gamma(\omega) = 4\pi^2 \alpha \omega S_{E1}(\omega)$$

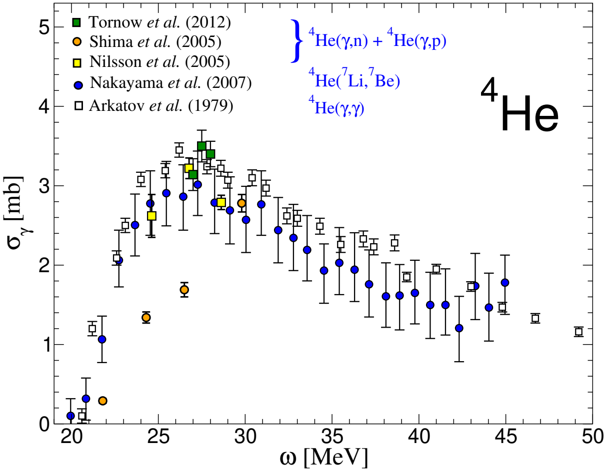

Determine $S_{\hat{O}}$ from photo-nuclear reaction experiments

$$\sigma_\gamma(\omega) = 4\pi^2 \alpha \omega S_{E1}(\omega)$$

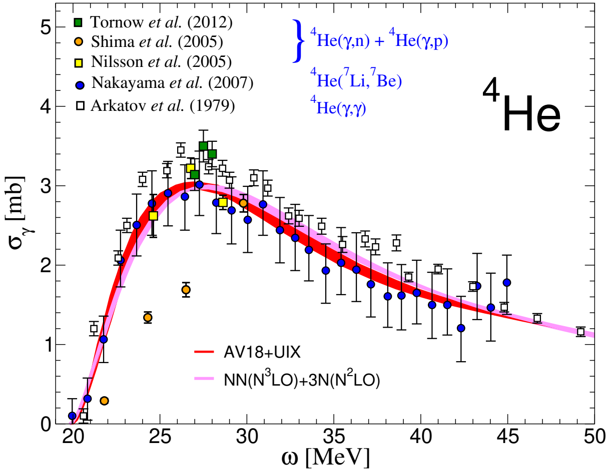

Ab-initio calculations of nuclear polarizability $\delta_{\rm pol}$

- $\mu^{2,3}$H, $\mu^{3,4}$He$^+$:
  - Numerical ab-initio methods

    Effective Interaction Hyperspherical Harmonics Expansion
    Lorentz Integral Transform (response function)
    Lanczos Algorithm (sum rules)

    bound state $\rightarrow$ resonance/continuum
  - Nuclear potentials

    AV18+UIX
    χEFT NN(N^{3}LO)+NNN(N^{2}LO)
    Analyze nuclear-theory uncertainty by comparing $\delta_{\rm pol}$ from different potential models

CJ, Nevo-Dinur, Bacca, Barnea, PRL 111 (2013) 143402
Hernandez, CJ, Bacca, Nevo-Dinur, Barnea, PLB 736 (2014) 344
Nevo Dinur, CJ, Bacca, Barnea, PLB 755 (2016) 380
Hernandez, Ekström, Nevo Dinur, CJ, Bacca, Barnea, PLB 788 (2018) 377
CJ, Bacca, Barnea, Hernandez, Nevo-Dinur, JPG 45 (2018) 093002

Hyperspherical harmonic basis (few-body methods)

For heavier nucleus, one needs to go beyond the Lippmann-Schwinger equation and adopt a more powerful few-body methods to deal with bound-state and continuum-state few-body systems.

- Solve in the 3-body CM frame

  $[T+V]\psi(\vec{\eta}_1,\vec{\eta}_2)=E\psi(\vec{\eta}_1,\vec{\eta}_2)$

- Use hyperspherical coordinates

  $\rho=\sqrt{\eta_1^2+\eta_2^2}$, $\Omega=[\theta_1,\phi_1,\theta_2,\phi_2,\arctan(\frac{\eta_2}{\eta_1})]$

  $T=T_\rho+\hat{K}^2/\rho^2$

- hyperspherical harmonic basis expansion

$$\psi(\vec{\eta}_1,\vec{\eta}_2)\sim\sum_{[K]}^{K_{max}}R_{[K]}(\rho)\,\mathcal{Y}_{[K]}(\Omega)$$

$\hat{K}^2\mathcal{Y}_{[K]}(\Omega)=K(K+4)\mathcal{Y}_{[K]}(\Omega)$

3-body problem

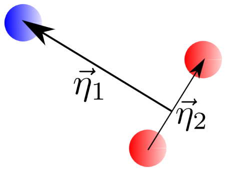

Hyperspherical harmonics basis expansion

$$|\psi\rangle = \sum_{K}^{K_{max}} c_K \, \mathrm{HH}(K)$$

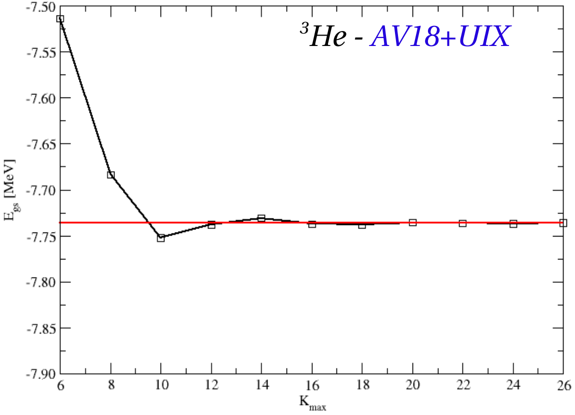

Lanczos algorithm for sum rules

- $\delta_{\rm pol} \Longrightarrow$ energy-dependent nuclear sum rules

$$I_{\hat{O}} = \int_0^{\infty} d\omega \, S_{\hat{O}}(\omega) \, g(\omega)$$

- Lanczos method can directly calculate I_O without explicitly knowing $S_{\hat{O}}(\omega)$.

- Map Hamiltonian in recursive Krylov subspace

$$\{\phi_0, \phi_1, \cdots, \phi_M\}$$

$$b_{i+1}|\phi_{i+1}\rangle = \hat{H}|\phi_i\rangle - a_i|\phi_i\rangle - b_i|\phi_{i-1}\rangle$$

$$|\phi_{-1}\rangle = 0; \quad |\phi_0\rangle = \hat{O}|\Psi_0\rangle; \quad \langle\phi_i|\phi_j\rangle = \delta_{ij}$$

- $I_{\hat{O}}$ converges when increasing Lanczos steps

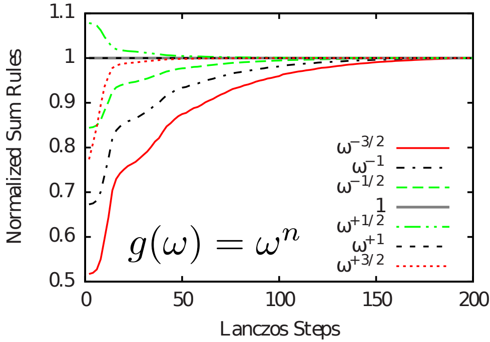

Nevo-Dinur, Barnea, CJ, Bacca, PRC **89**, 064317 (2014)

TPE & nuclear polarizability: nuclear-model uncertainty

δ_{TPE} in $\mu\,^3$He$^+$

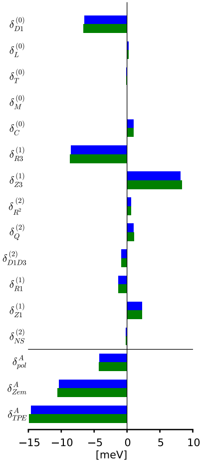

	AV18/UIX	χEFT
$\delta^{(0)}_{D1}$	-6.479	-6.633
$\delta^{(0)}_{L}$	0.232	0.240
$\delta^{(0)}_{T}$	-0.103	-0.107
$\delta^{(0)}_{M}$	0.006	0.006
$\delta^{(0)}_{C}$	1.000	1.020
$\delta^{(1)}_{R3}$	-8.539	-8.711
$\delta^{(1)}_{Z3}$	8.100	8.327
$\delta^{(2)}_{R^2}$	0.632	0.654
$\delta^{(2)}_{Q}$	1.015	1.038
$\delta^{(2)}_{D1D3}$	-0.841	-0.862
$\delta^{(1)}_{R1}$	-1.294	-1.314
$\delta^{(1)}_{Z1}$	2.256	2.291
$\delta^{(2)}_{NS}$	-0.193	-0.199
δ^{A}_{pol}	-4.208	-4.250
δ^{A}_{Zem}	-10.356	-10.618
δ^{A}_{TPE}	-14.564	-14.868

$\delta_{\mathrm{TPE}} = -14.72$ meV $\pm 1.5\%(1\sigma)$

δ_{TPE} in $\mu\,^4$He$^+$

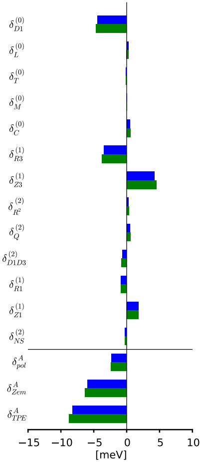

	AV18/UIX	χEFT
$\delta^{(0)}_{D1}$	-4.418	-4.701
$\delta^{(0)}_{L}$	0.289	0.308
$\delta^{(0)}_{T}$	-0.126	-0.134
$\delta^{(0)}_{M}$	0.008	0.006
$\delta^{(0)}_{C}$	0.519	0.553
$\delta^{(1)}_{R3}$	-3.442	-3.717
$\delta^{(1)}_{Z3}$	4.183	4.526
$\delta^{(2)}_{R^2}$	0.259	0.324
$\delta^{(2)}_{Q}$	0.484	0.561
$\delta^{(2)}_{D1D3}$	-0.666	-0.784
$\delta^{(1)}_{R1}$	-0.848	-0.874
$\delta^{(1)}_{Z1}$	1.753	1.811
$\delta^{(2)}_{NS}$	-0.279	-0.293
δ^{A}_{pol}	-2.284	-2.414
δ^{A}_{Zem}	-5.936	-6.337
δ^{A}_{TPE}	-8.220	-8.751

$\delta^{A}_{\mathrm{TPE}} = -8.49$ meV $\pm 4.4\%(1\sigma)$

TPE & nuclear polarizability: other uncertainty

Numerical uncertainty

- convergence of EIHH model space (μ^4He$^+$)

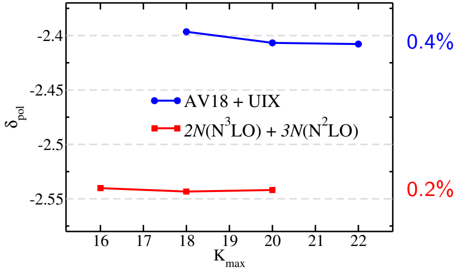

Atomic-physics uncertainty

- $(Z\alpha)^6$ correction three-photon exchange
- relativistic and Coulomb distortion effects to sum rules beyond E1
- higher-order nucleonic-structure corrections
- Overall atomic-physics uncertainty
  - 1.5% in μ^3He$^+$
  - 1.3% in μ^4He$^+$

- Combine all uncertainties:

  $\delta_{\rm TPE}(\mu^3{\rm He}^+) = -14.72$ meV $\pm 2.1\%$

  $\delta_{\rm TPE}(\mu^4{\rm He}^+) = -8.49$ meV $\pm 4.6\%$

- The TPE prediction fulfills the 5% accuracy requirements from $\mu^{3,4}$He$^+$ experiments

Nuclear charge radii from Lamb shifts in μ^2H and $\mu^{3,4}$He

- Our predictions of nuclear TPE effects have been used by CREMA to extract nuclear charge radii from Lamb shift measurements
- Theoretical uncertainties in TPE effects dominate the error in the extracted nuclear charge radii

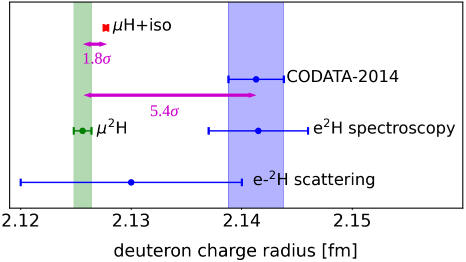

$$r_d = 2.12562(13)_{\rm exp}(77)_{\rm theo}\ \text{fm}$$

Pohl, *et al.*, Science (2016)

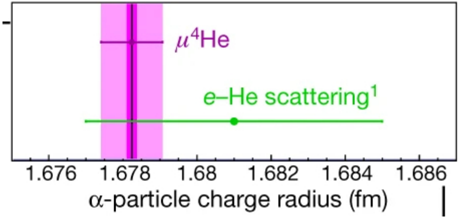

$$r_\alpha = 1.67824(13)_{\rm exp}(82)_{\rm theo}\ \text{fm}$$

Krauth et al., Nature (2021)

TPE theory:
Hernandez, CJ, Bacca, Nevo-Dinur, Barnea, PLB 736 (2014) 344; PRC 100 (2019) 064315 (μ^2H)
Hernandez, Ekström, Nevo Dinur, CJ, Bacca, Barnea, PLB 788 (2018) 377 (μ^2H)
CJ, Nevo-Dinur, Bacca, Barnea, PRL 111 (2013) 143402 (μ^4H)
CJ, Bacca, Barnea, Hernandez, Nevo-Dinur, JPG 45 (2018) 093002 ($\mu^{2,3}$H, $\mu^{3,4}$He$^+$)

Nuclear charge radii from Lamb shifts in μ^2H and $\mu^{3,4}$He

- Our predictions of nuclear TPE effects have been used by CREMA to extract nuclear charge radii from Lamb shift measurements
- Theoretical uncertainties in TPE effects dominate the error in the extracted nuclear charge radii

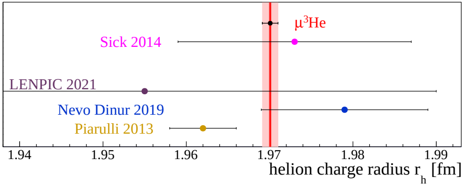

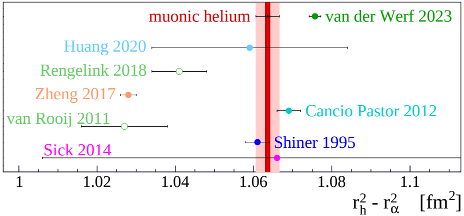

$$r_h = 1.97007(12)_{\text{exp}}(93)_{\text{theo}} \text{ fm}$$

$$r_h^2 - r_\alpha^2 = 1.0636(6)_{\text{exp}}(30)_{\text{theo}} \text{ fm}^2$$

Schuhmann et al. (CREMA) arXiv:2305.11679

TPE theory:
Nevo Dinur, CJ, Bacca, Barnea, PLB 755 (2016) 380 (μ^3H, μ^3He$^+$)
CJ, Bacca, Barnea, Hernandez, Nevo-Dinur, JPG 45 (2018) 093002 ($\mu^{2,3}$H, $\mu^{3,4}$He$^+$)

Higher-order EM operators

- higher-order currents are constructed from chiral EFT
- relativistic and meson-exchange currents (RC+MEC)

$$\mathbf{j} = \sum_{n=-2}^{+1} \mathbf{j}^{(n)}, \quad \rho = \sum_{n=-3}^{+1} \rho^{(n)}$$

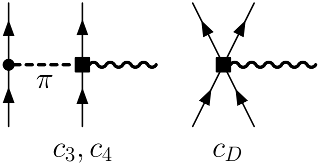

Pastore *et al.*, PRC '08,'09,'11; Kölling *et al.*, PRC '09,'11

		r_d [fm]	Q_d [fm^2]
N3LO	Impulse Approx	1.976	0.2750
	+RC+MEC	1.976	0.2851
AV18	Impulse Approx	1.969	0.2697
	+RC+MEC	1.969	0.2806
Experiment		1.9751(8)	0.28578(3)

Piarulli *et al.* PRC '13

Higher-order EM operators

- higher-order currents are constructed from chiral EFT
- relativistic and meson-exchange currents (RC+MEC)

$$\mathbf{j} = \sum_{n=-2}^{+1} \mathbf{j}^{(n)}, \quad \rho = \sum_{n=-3}^{+1} \rho^{(n)}$$

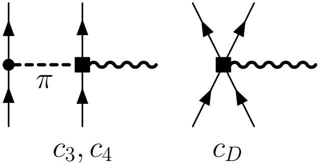

Pastore *et al.*, PRC '08,'09,'11; Kölling *et al.*, PRC '09,'11

		r_d [fm]	Q_d [fm^2]
N3LO	Impulse Approx	1.976	0.2750
	+RC+MEC	1.976	0.2851
AV18	Impulse Approx	1.969	0.2697
	+RC+MEC	1.969	0.2806
Experiment		1.9751(8)	0.28578(3)

Piarulli *et al.* PRC '13

- Test RC+MEC contributions to δ_{Zem} & other EM moments

RC+MEC contributions to EM moments in ^{2}H

Method	R_E [fm]	$\langle R_E^3 \rangle_{(2)}$ [fm^3]	$\langle R_E^4 \rangle$ [fm^4]	R_Z [fm]	R_M [fm]	μ [μ_N]
IA	1.953(1)	27.56(20)	32.5(1.3)	2.598(1)	2.103(1)	-1.757(1)
IA+RC	1.975(1)	28.44(20)	33.6(1.3)	2.621(1)	2.116(1)	-1.737(1)
TOT	1.979(1)(10)	28.58(66)(13)	33.8(1.5)(2)	2.539(3)(19)	1.991(1)(31)	-2.093(1)(55)
Exp.	1.973(14)	28.15(70)	32.9(1.60)	2.528(16)	1.976(47)	-2.127

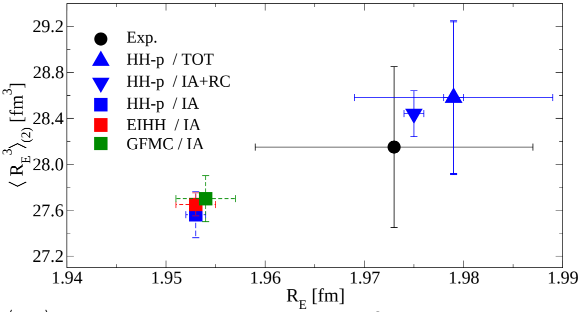

$$\left\langle R_E^3 \right\rangle_{(2)} = \iint d\boldsymbol{r} d\boldsymbol{r}' \rho_E(\boldsymbol{r}) \rho_E(\boldsymbol{r}') |\boldsymbol{r}-\boldsymbol{r}'|^3$$

electric Zemach moment

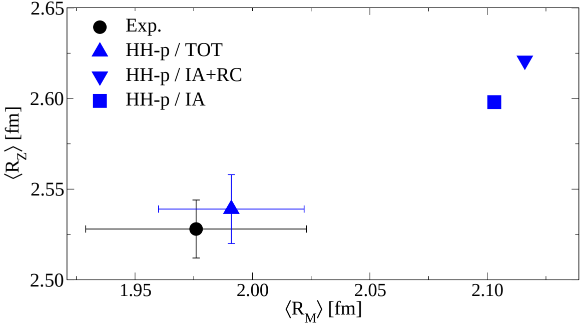

$$R_Z = \iint d\boldsymbol{r} d\boldsymbol{r}' \rho_E(\boldsymbol{r}) \rho_M(\boldsymbol{r}') |\boldsymbol{r}-\boldsymbol{r}'|$$

magnetic Zemach moment

Nevo-Dinur, Hernandez, Bacca, Barnea, CJ, Pastore, Piarulli, Wiringa, PRC 99, 034004 (2019)

Nuclear Zemach radii from hyperfine splittings in muonic atoms

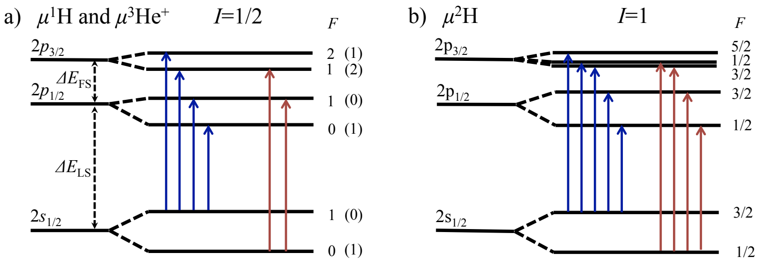

- Zemach radius R_Z is determined by both nuclear charge and magnetic densities

$$R_Z = \iint d\boldsymbol{r} d\boldsymbol{r}' \rho_E(\boldsymbol{r}) \rho_M(\boldsymbol{r}') |\boldsymbol{r} - \boldsymbol{r}'|$$

- CREMA (PSI): determine R_Z from measured HFS in muonic atoms

Status of theoretical and experimental studies

- TPE effects dominate the discrepancy between measured and QED-predicted HFS
- Accidental agreement between the predicted and measured TPE effects in ^{2}H HFS?
- Large discrepancies between the calculated and experimental TPE effects in μ^2H HFS
- Current theories do not rigorously treat nuclear excitations in TPE to HFS.

e^2H 1S $E_{HFS}(2\gamma)$ [kHz]	
$\nu_{\rm exp} - \nu_{\rm qed}$	45 [1]
Khriplovich, Milstein 2004	43 (model dependent)
Friar 2005	46 $(+18)$
	$(1N$ pol/recoil)

μ^2H 2S $E_{HFS}(2\gamma)$ [meV]	
$\nu_{\rm exp} - \nu_{\rm qed}$	0.0966(73) [2]
Kalinowski, Pachucki 2018	0.0383

[1] Wineland, Ramsey, PRA (1972)
[2] Pohl et al., Science (2016)

TPE contributions to HFS in ^{2}H and μ^2H

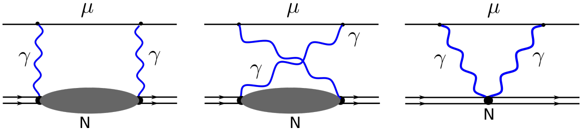

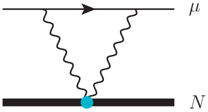

- TPE effects

$$E_{\rm TPE} = E_{\rm el} + E_{\rm pol} + E_{\rm 1N}$$

- elastic: $F_c(q)$, $F_m(q)$, $F_Q(q)$
- inelastic: vector polarization
- $E_{\rm 1N}$: single-nucleon TPE

$$\delta^{(0,1)}_{\rm pol} \quad \propto \quad \int d\omega \int dq h^{(0,1)}(\omega,q) S^{(0,1)}(\omega,q)$$

$$S^{(0)}(\omega,q) \quad = \quad -\frac{1}{q^2}{\rm Im} \sum_{N\neq N_0} \int \frac{d\hat{q}}{4\pi} \langle N_0 II| \left[\vec{q}\times\vec{J}^{\dagger}_m(\vec{q})\right]_3 |N\rangle\langle N|\rho(\vec{q})|N_0 II\rangle \delta(\omega - \frac{q^2}{2m_A} - \omega_N)$$

$$S^{(1)}(\omega,q) \quad = \quad -{\rm Im} \sum_{N\neq N_0} \int \frac{d\hat{q}}{4\pi} \epsilon^{3jk} \langle N_0 II|\vec{J}^{\dagger}_{m,j}(\vec{q})|N\rangle\langle N|\vec{J}_{c,k}(\vec{q})|N_0 II\rangle |N_0 II\rangle \delta(\omega - \frac{q^2}{2m_A} - \omega_N)$$

- Plan A: χEFT (in progress)
- Plan B: $\not\pi$EFT <u>CJ</u>, Zhang, Platter, arXiv:2311.13585

Pionless effective field theory

- Contact NN and NNN interactions (without pion)
- Predictions require only a few input parameters:a_t, r_t at NNLO (4% accuracy)

$$
\begin{aligned}
\mathcal{L} \quad = \quad & N^\dagger \left[i\partial_0 + \frac{\nabla^2}{2M} \right] N - C_0 \left(N^T P_i N \right)^\dagger \left(N^T P_i N \right) \\
& + \frac{1}{8} C_2 \left[\left(N^T P_i N \right)^\dagger \left(N^T \overleftrightarrow{\nabla}^2 P_i N \right) + h.c. \right] - \frac{1}{16} C_4 \left(N^T \overleftrightarrow{\nabla}^2 P_i N \right)^\dagger \left(N^T \overleftrightarrow{\nabla}^2 P_i N \right) \\
& + \frac{1}{4} C_0^{(sd)} \left\{ \left(N^T P^i N \right)^\dagger \left[N^T P^j \left(\overleftrightarrow{\nabla}_i \overleftrightarrow{\nabla}_j - \frac{1}{3} \delta_{ij} \overleftrightarrow{\nabla}^2 \right) N \right] + \text{h.c.} \right\}
\end{aligned}
$$

Kaplan, Savage, Wise, Nuclear Physics B 534 (1998) 329

- reproduce np $3S1$ phase shift

$$
p \cot \delta_t(p) = -\gamma + \frac{\rho}{2}(p^2 + \gamma^2) + \cdots
$$

$$
\begin{aligned}
C_0 &= C_{0,-1} + C_{0,0} + C_{0,1} + \cdots \\
C_2 &= C_{2,-2} + C_{2,-1} + \cdots \\
C_4 &= C_{4,-3} + \cdots
\end{aligned}
$$

$$
C_{0,-1} = -\frac{4\pi}{m_N}\frac{1}{\mu-\gamma}, \qquad C_{0,0} = \frac{2\pi}{m_N}\frac{\rho\gamma^2}{(\mu-\gamma)^2},
$$

$$
C_{0,1} = -\frac{\pi}{m_N}\frac{\rho^2\gamma^4}{(\mu-\gamma)^3}, \qquad C_{2,-2} = \frac{2\pi}{m_N}\frac{\rho}{(\mu-\gamma)^2},
$$

$$
C_{2,-1} = -\frac{2\pi}{m_N}\frac{\rho^2\gamma^2}{(\mu-\gamma)^3}, \qquad C_{4,-3} = -\frac{\pi}{m_N}\frac{\rho^2}{(\mu-\gamma)^3}
$$

$$
C_0^{(sd)} = -\frac{6\sqrt{2}\pi}{m_N \gamma^2 (\mu-\gamma)} \eta_{sd} \qquad \leftarrow \quad \text{asymptotic D-S ratio}
$$

Pionless effective field theory

- Solve Lippmann-Schwinger equation
- t-matrix $\mathcal{A}_n$ in perturbation:

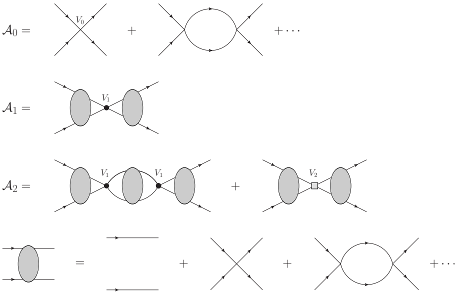

- on-shell:

$$\mathcal{A}_t(p,p;E) = -\frac{4\pi}{m_N}\frac{1}{\gamma+ip}\left[1+\frac{\rho}{2}(\gamma-ip)+\frac{\rho^2}{4}(\gamma-ip)^2\right]$$

- off-shell:

$$\mathcal{A}_t^{(0)}(k,p;E) = -\frac{4\pi}{m_N}\frac{1}{\gamma+ip}$$

$$\mathcal{A}_t^{(1)}(k,p;E) = -\frac{2\pi}{m_N}\frac{\rho}{\gamma+ip}\left[\gamma-ip+\frac{1}{2(\gamma-\mu)}\left(k^2-p^2\right)\right]$$

$$\mathcal{A}_t^{(2)}(k,p;E) = -\frac{\pi}{m_N}\frac{\rho^2}{\gamma+ip}\left[(\gamma-ip)^2+\frac{\gamma-ip}{\gamma-\mu}\left(1+\frac{\gamma+ip}{\gamma-\mu}\right)\frac{k^2-p^2}{2}\right]$$

$\not{\pi}$EFT calculation of TPE effects to Lamb shift in $^2\mu$H

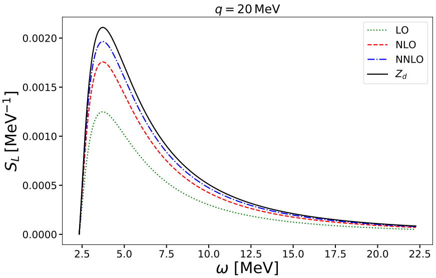

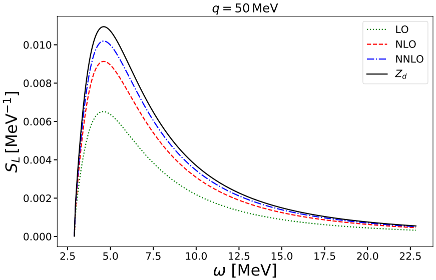

- longitudinal response function shows order-by-order convergence in $\not{\pi}$EFT
- TPE predicted in $\not{\pi}$EFT at NNLO agrees well the χEFT calculations

δ_{pol}	non-relativistic kernel	relativistic kernel
$\not{\pi}$EFT	-1.605	-1.574
χEFT	-1.590	-1.560

Emmons, CJ*, Platter, J. Phys. G 48, 035101 (2021)

$\not{\pi}$EFT calculation of TPE effects to HFS in ^{2}H and ${}^2\mu$H

- Contributions from one-body charge density, convection and magnetic curents ρ_E, $\vec{J}_c$, $\vec{J}_m$
-

$$\begin{aligned}\mathcal{L}_{\text{EM},1b} =& -eN^\dagger \frac{1+\tau_3}{2} N A_0 \\ & - \frac{ie}{2m_N}\left[N^\dagger \overleftrightarrow{\nabla} \frac{1+\tau_3}{2} N\right]\cdot \vec{A} \\ & + \frac{e}{2m_N} N^\dagger \left(\kappa_0 + \kappa_1 \tau_3\right) \vec{\sigma}\cdot \vec{B} N\end{aligned}$$

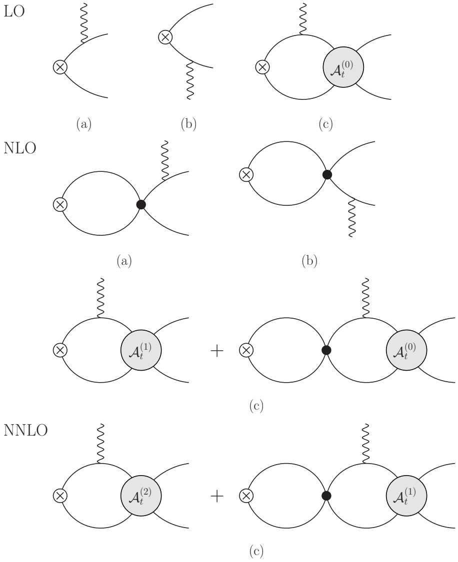

$\not{\pi}$EFT calculation of TPE effects to HFS in ^{2}H and $^2\mu$H

- $\vec{J}_c$ (NLO), $\vec{J}_m$ (NNLO) two-nucleon currents

$$\mathcal{L}_{2,C} = ie\frac{C_2}{4}\left[(N^T P_i N)^\dagger (N^T \overleftrightarrow{\nabla} P_i \tau_3 N) + \text{h.c.}\right] \cdot \vec{A}$$

$$\mathcal{L}_{2,B} = -ieL_2\epsilon_{ijk}\left(N^T P_i N\right)^\dagger \left(N^T P_j N\right) B_k + \text{h.c.}$$

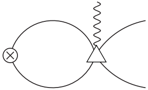

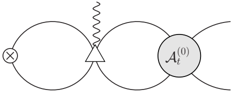

- np S-D mixing at NNLO

$$\mathcal{L}_{2,Q} = -eL_Q\left(N^T P_i N\right)^\dagger \left(N^T P_j N\right)\left(\nabla^i\nabla^j - \frac{1}{3}\nabla^2\delta_{ij}\right) A_0$$

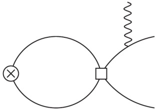

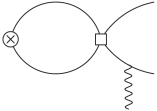

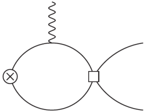

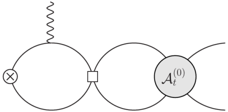

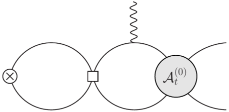

Response functions in $\not\pi$EFT

- $S^{(0)}(\omega, q)$: charge-magnetic transition (LO)
- $S^{(1)}(\omega, q)$: convection-magnetic transition (NLO)
- $S^{(0)}_{\mathrm{sd}}(\omega, q)$: S-D mixing correction to $S^{(0)}$ (NNLO)
- systematic order-by-order convergence

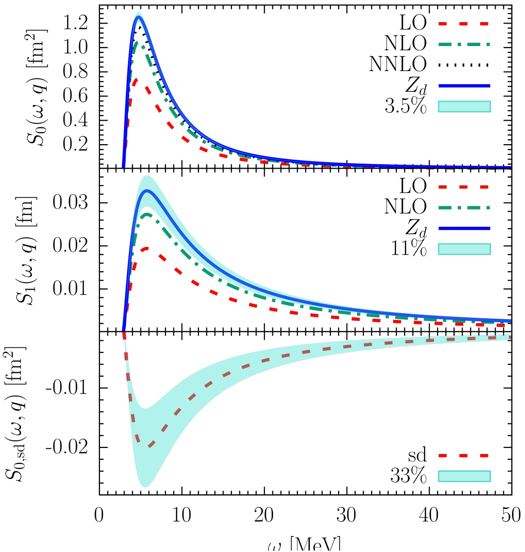

TPE corrections to HFS in ^{2}H and μ^2H

	^{2}H (1S)	μ^2H (1S)	μ^2H (2S)
$E_{1\mathrm{p}}$ (Antognini 2022)	$-35.54(8)$	$-1.018(2)$	$-0.1272(2)$
$E_{1\mathrm{n}}$ (Tomalak 2019)	$9.6(1.0)$	$0.08(3)$	$0.010(4)$
E_{el}	$-41.9(1.5)$	$-0.985(34)$	$-0.123(4)$
E_{pol}	$109.8(3.8)$	$2.86(10)$	$0.358(13)$
E_{TPE}	kHz	meV	meV
This work	$41.7(2.6)$	$0.940(73)$	$0.118(9)$
Khriplovich, Milstein 2004	43		
Friar, Payne 2005 $_{\mathrm{mod}}$	64.5		
Kalinowskim, Pauckci 2018		$0.304(68)$	$0.0383(86)$
$\nu_{\mathrm{exp}} - \nu_{\mathrm{qed}}$	45		$0.0966(73)$

- Consistent with $\nu_{\mathrm{exp}} - \nu_{\mathrm{qed}}$ within $1.4 - 1.7\sigma$
- Further improvement on accuracy in nuclear theory is demanding
- Uncertainty in E_{1p} and E_{1n} can be larger than expected! (χPT v.s. dispersion)

CJ, Zhang, Platter, arXiv:2311.13585

Conclusion

- radius puzzle & spectroscopy in hydrogen-like atoms
  - Challenge higher-order QED theory
  - TPE effects connect atomic transition with photo-nuclear reaction
  - Use low-energy nuclear theory to probe precision physics
- TPE effects to Lamb shift
  - determine nuclear charge radii
  - Ab inito calculations improve theoretical accuracy to percentage
  - more accurate than extracting information from photonuclear reaction data
- TPE effects to hyperfine splitting
  - determine nuclear magnetic structure
  - Ab initio theory to determine TPE effects to HFS
  - further improve accuracy in nuclear theory (χEFT, or $\not\pi\mathrm{EFT}$ at N^{3}LO)
  - uncertainty in nucleonic TPE needs to be reanalyzed
  - Future extension to study TPE effects to HFS in μ^3He, $e^{6,7}$Li

Collaborators

O.J. Hernandez, S. Bacca, T. Richardson	Johannes Gutenberg-Universität Mainz
N. Nevo-Dinur	TRIUMF
N. Barnea	Hebrew University of Jerusalem
A. Ekström	Chalmers University of Technology
S. Pastore, M. Piarulli	Washington University
R.B. Wiringa	Argonne National Laboratory
J.L. Bonilla, L. Platter	University of Tennessee, Knoxville
S.B. Emmons	Carson-Newman University

Lamb Shift & QED

- **Dirac theory:** $2s_{1/2}$ & $2p_{1/2}$ levels of hydrogen are degenerate
- **Lamb & Retherford Experiments (1947):**

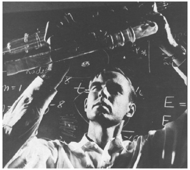

$$\delta E_{LS} = E(2s_{1/2}) - E(2p_{1/2}) = 1057.8(1)\ \mathrm{MHz}$$

PHYSICAL REVIEW VOLUME 72, NUMBER 3 AUGUST 1, 1947

Fine Structure of the Hydrogen Atom by a Microwave Method* **

WILLIS E. LAMB, JR. AND ROBERT C. RETHERFORD
Columbia Radiation Laboratory, Department of Physics, Columbia University, New York, New York

(Received June 18, 1947)

- **Lamb shift gave the main impetus to the development of modern QED.**
- **Bethe Theory (1947):**
  - combine non-relativistic QM, 2nd order perturbation theory, & Kramers' QED renormalization concept
  - calculate the QED self-energy correction to account for Lamb's discovery

PHYSICAL REVIEW VOLUME 72, NUMBER 4 AUGUST 15, 1947

The Electromagnetic Shift of Energy Levels

H. A. BETHE
Cornell University, Ithaca, New York

(Received June 27, 1947)

BY very beautiful experiments, Lamb and Retherford[1] have shown that the fine struc- explained by a nuclear interaction of reasonable magnitude, and Uehling[5] has investigated the

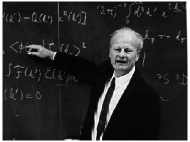

Radiative Correction at $\mathcal{O}(e^4)$ in QED

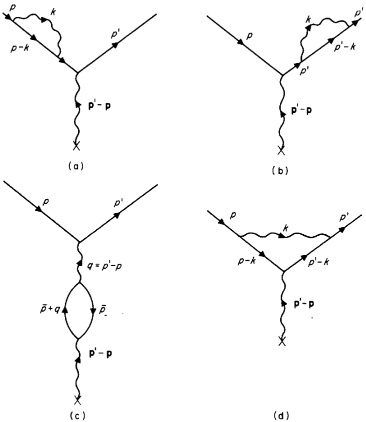

Fig. 9.2. The four contributions to the second-order radiative corrections to electron scattering.

Mandl, Shaw, Quantum Field Theory;
Aitchison, Hey, Gauge Theories in Particle Physics

(a,b) electron self-energy

(c) photon self-energy (vacuum polarization)

(d) vertex correction

- Consequence of Radiative Correction:
  - **Renormalization:**
    field strength;
    lepton mass;
    photon self-energy;
    lepton charge
  - **Gauge invariance requires:** $m_\gamma = 0$
  - **Charge universality**: $e_\mu = e_e$

Lamb Shift & Radiative Correction Theory

- **In $e - p$ scattering, radiative correction only contributes to the mass and charge renormalization.**
- **In eH bound states, radiative correction produces level shift**
- **In Bethe's calculation:**
  - **Level shift is the difference between self-energies of bound and free electrons**
  - Electron self-energy correction can be evaluated by 2nd order perturbation in electric dipole approximation

$$\delta E(nl) = -\sum_{\lambda} \sum_{r=1,2} \left(\frac{e}{m}\right)^2 \int \frac{d^3k}{(2\pi)^3} \frac{|\langle \lambda | \boldsymbol{\epsilon}_r(\boldsymbol{k}) \cdot \boldsymbol{p} | nl \rangle|^2}{2k(E_\lambda + k - E_n)}$$

$$= -\frac{1}{6\pi^2} \left(\frac{e}{m}\right)^2 \sum_{\lambda} |\langle \lambda | \boldsymbol{p} | nl \rangle|^2 \int_0^\infty dk \frac{k}{E_\lambda + k - E_n}$$

← linear divergence at $k \to \infty$

$|\lambda\rangle$: intermediate atomic states

Bethe, Phys. Rev. 72, 339 (1947)
Mandl, Shaw, Quantum Field Theory

Lamb Shift & Radiative Correction Theory

- **In Bethe's calculation:**
  - For a free electron, the self-energy provides the **mass renormalization**
  - The corresponding **mass correction** for the electron in the $|nl\rangle$ state is

$$\delta E_f(nl) == -\frac{1}{6\pi^2}\left(\frac{e}{m}\right)^2 \sum_\lambda |\langle\lambda|\boldsymbol{p}|nl\rangle|^2 \int_0^\infty dk \leftarrow \textbf{linear divergence at } k \rightarrow \infty$$

  - physical electron mass is used in $\delta E(nl)$, the mass correction is already included.
  - **observed level shift $\boldsymbol{\Delta E(nl)}$:** difference between self-energies of bound and free electrons

$$\begin{aligned}\Delta E(nl) =& \delta E(nl) - \delta E_f(nl)\\ =& -\frac{1}{6\pi^2}\left(\frac{e}{m}\right)^2 \sum_\lambda |\langle\lambda|\boldsymbol{p}|nl\rangle|^2 \int_0^\infty dk \frac{E_\lambda - E_n}{E_\lambda + k - E_n}\end{aligned}$$

  - After numerical evaluation, Bethe found that

$$E(2s_{1/2}) - E(2p_{1/2}) = 1040 \text{ MHz}$$

    - in remarkable agreement with experiment value $1057.8(1)$ MHz

Bethe, Phys. Rev. 72, 339 (1947)
Mandl, Shaw, Quantum Field Theory

Lamb Shift & Radiative Correction Theory

- **Photon vacuum polarization correction (Uehling Effect):**
  - Introduce a short-range modification to the Coulomb potential between ep

$$-\frac{\alpha}{r} \to -\frac{\alpha}{r} - \frac{4\alpha^2}{15\pi m_e^2}\delta^3(\boldsymbol{r})$$

  - The vacuum polarization makes a 1st order perturbative correction to atomic levels

$$\Delta E_{\mathrm{vp}}(nl) \quad = \quad \langle nl|V_{vp}|nl\rangle = -\frac{4\alpha^2}{15 m_e^2}|\phi_{nl}(0)|^2 = -\frac{8\alpha^3}{15\pi n^3}\mathrm{Ry}\,\delta_{l0}$$

  - Uehling effect's correction in hydrogen is subleading

$$E(2s_{1/2}) - E(2p_{1/2}) = -27\ \mathrm{MHz}$$

- **Lamb Shift offers an important test ground for bound state QED**

Beth, Phys. Rev. 72, 339 (1947)
Mandl, Shaw, Quantum Field Theory

Lamb Shift in Muonic Hydrogen

- **Muon mass is ~210 times of electron mass**
- **Radiative Corrections in muonic hydrogen indicate a different hierarchy**

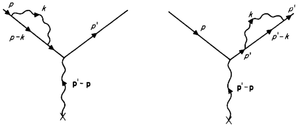

- **Lepton Self Energy:**
  - enhanced by the factor (m_μ/m_e)
  - $\Delta E_{2s,se}(\mu H) \approx 210\ \Delta E_{2s,se}(eH) \approx 220\ \mathrm{GHz}$

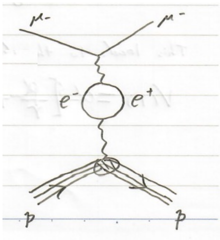

- **Vacuum Polarization:**
  - enhanced by the factor $(m_\mu/m_e)^3$
  - $\Delta E_{2s,vp}(\mu H) \approx (210)^3\ \Delta E_{2s,vp}(eH) \approx -250\ \mathrm{THz}$

- **Vacuum polarization (Uehling effect) dominates in Lamb shift in muonic hydrogen**